Preprints, 22th Conf. on Weather Analysis and Forecasting
and 18th Conf. on Numerical Weather Prediction
Amer. Meteor. Soc., Park City, UT, 25-29 June 2007

3B.1 CAPS REALTIME STORM-SCALE ENSEMBLE AND HIGH-RESOLUTION FORECASTS AS PART OF THE NOAA HAZARDOUS WEATHER TESTBED 2007 SPRING EXPERIMENT

Ming Xue[1], Fanyou Kong[1], Daniel Weber[1] Kevin W. Thomas[1], Yunheng Wang[1], Keith Brewster[1], Kelvin K. Droegemeier[1], John Kain[2], Steve Weiss[3], David Bright[3], Matt Wandishin[4], Mike Coniglio[5] and Jun Du[6]

[1]Center for Analysis and Prediction of Storms, University of Oklahoma
[2]National Severe Storms Laboratory, NOAA
[3]Storm Prediction Center/NCEP, NOAA
Norman, Oklahoma
[4]Department of Atmospheric Physics, University of Arizona, Tucson, Arizona
[5]Cooperative Institute for Mesoscale Meteorological Studies, Norman, Oklahoma
[6]Environmental Modeling Center/NCEP, NOAA, Maryland

1. Introduction

Accurate prediction of convective-scale hazardous weather continues to be a major challenge, because of the small spatial and temporal scales of the associated weather systems, and the inherent nonlinearity of their dynamics and physics. So far, the resolutions of operational numerical weather prediction (NWP) models remain too low to resolve explicitly convective-scale systems, which constitutes one of the biggest sources of uncertainty and inaccuracy of the quantitative prediction. These and other uncertainties as well as the high-nonlinearity of the weather systems at such scales render probabilistic forecast information afforded by high-resolution ensemble forecasting systems especially valuable to operational forecasting.

Under the support of the NOAA CSTAR (Collaborative Science, Technology, and Applied Research) Program with leverage on the support of the NSF Large ITR LEAD (Linked Environment for Atmospheric Discovery) project, the Center for Analysis and Prediction of Storms (CAPS) at the University of Oklahoma is carrying out a three year project, in collaborations with the NOAA Hazardous Weather Testbed (HWT, see, e.g., Weiss et al. 2007) in Norman Oklahoma, to develop, conduct, and evaluate realtime high-resolution ensemble and deterministic forecasts for convective-scale hazardous weather. The realtime forecasts, together with retrospective analyses using the real time data, aim to address scientific issues including: (1) the values and cost-benefits of storm-scale ensemble versus coarser-resolution short-range ensembles and even-higher-resolution deterministic forecast; (2) suitable perturbation methods for storm-scale ensemble, among breeding, ETKF (ensemble Transform Kalman filter), physics perturbations, and multi-model ensemble; (3) proper handling and use of lateral and lower boundary perturbations; (4) the value and impact of assimilating high-resolution data including those from WSR-88D radars; (5) the most effective ensemble forecast products for the storm scales; and (6) the impact of such unique products on realtime forecasting and warning.

[1] *Corresponding author address:*
Dr. Ming Xue, Center for Analysis and Prediction of Storms, University of Oklahoma, Norman OK 73072; e-mail: mxue@ou.edu

2. 2007 Spring Forecasts

In the first year of the three-year CSTAR-supported project, in the spring of 2007, CAPS produced daily 33-hour 10-member 4-km-resolution storm-scale ensemble forecasts (SSEF), as contributions to the HWT 2007 Spring Experiment (Weiss et al. 2007). At the same time, a single 33-hour 2-km deterministic forecast (ARW2) was produced over the same domain that covers two thirds of the continental US (Fig. 1).

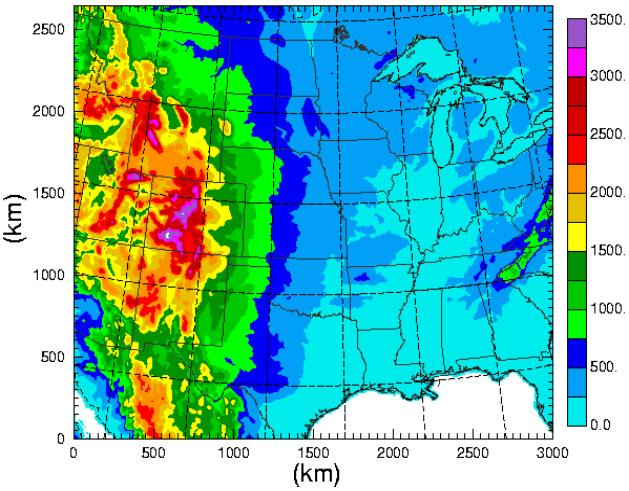

Fig. 1. The domain of the 2-km HR and 4-km storm-scale ensemble forecasting (SSEF) models using WRF. Color shaded contours for terrain elevation are shown.

This domain is of the same size as the one CAPS used during the 2005 Spring Experiment (e.g., Kain et al. 2007), when a single 2-km WRF-ARW forecast was produced daily. The forecasts were initialized at 2100 UTC and extend to 0600 UTC of the third day (In UTC). The experiment started on April 15, 2007 and ended on June 8, 2007. The forecasts were produced Saturday through Thursday each week, for them to be used during the weekdays.

The CAPS forecasts used the WRF-ARW model and the ensemble included both initial condition (IC) and boundary condition (BC), and physics perturbations. The IC and BC perturbations were derived from the NCEP 2100 UTC SREF (Short-range Ensemble Forecast, Du et al. 2006) forecast cycle, with the IC of control member coming from the NAM 2100 UTC analysis on the 12 km grid. The pure physics-perturbation members are designed for easy identification of the characteristics of individual microphysics and PBL schemes within WRF.

All CAPS forecasts used the RRTM shortwave and Goddard long-wave radiation schemes, and the Noah land surface model. No cumulus parameterization is used. The subgrid-scale turbulence mixing is turned on without explicit computational mixing. The microphysics and PBL schemes are varied among the ensemble members while the 2-km and 4-km control member used the WRF single-moment 6-category microphysics (WSM6) scheme together with the Mellor-Yamada-Jancic (MYJ) PBL scheme. The physics options for other ensemble members are given in Table 1.

Four WRF members in the NCEP SREF were used to construct the perturbed IC and BC for some members of our SSEF system. Ensemble members N1 and P1, N2 and P2 (Table 1) are pairs that used negative and positive IC and BC perturbations from the WRF-ARW and WRF-NAM pairs of the SREF. Such perturbations were extracted from the SREF fields by taking the difference between the ensemble and control members then interpolating and adding the perturbation fields to the unperturbed IC and BC derived from the 12 km NAM analysis and forecasts. More details on the construction of perturbations can be found in Kong et al. (2007).

It is noted here that we used the pre-processing programs originally developed for the CAPS ARPS modeling system, for the creation of ICs and BCs for all WRF runs. They include programs that interpolate the NAM and SREF gridded data and construct the perturbations. This is accomplished by first performing all the preparation on the ARPS grid, which is set up to have identical horizontal grid space and map projection as WRF, then interpolating the ARP fields to the WRF grid (via program ARPS2WRF). All these programs support MPI. This is different from the common practice of using WRF SI (Standard Initialization) or the newer WPS (WRF Preprocessing System). Most of the ARPS-based pre- and post-processing programs had been tested intensively.

Using 66 processors of the Cray XT3 system at the Pittsburgh Supercomputing Center, each member of 33-hour forecast ensemble took 6.5 to 9.5 hours, with the differences being caused by the use of different physics options in the prediction model. The single 2-km 33-hour forecast using a 1501 × 1321 × 51 grid and 600 Cray XT3 processors took about 9 hours, including about 2-hours using by 3D data dumps at 5 minute intervals. The 5-min output were shipped back, via special links to the National Lamdarail Network at both the PSC and University of Oklahoma ends, to a supercomputer at the Oklahoma Supercomputer Center for Education and Research (OSCER). Reflectivity animations were created at OSCER that can be directly compared to movies created from the observed reflectivity mosaic of NSSL. Sustained throughput of over 150 mb/s was achieved via the Lamdarail.

Selected 2D fields and soundings were extracted from the 3D gridded output, and shipped to HWT for direct ingest into the N-AWIPS systems and for interactive manipulation and display by the forecast and evaluation teams. Additional post-processing and product generation from the ensemble output were also performed within the N-AWIPS.

During the 2007 HWT Spring Experiment, single WRF-ARW forecasts produced by NCAR at 3 km (ARW3) and by NSSL at 4 km (ARW4) horizontal resolutions, respectively, with about 35 vertical levels, together WRF-NMM forecasts produced by EMC/NCEP at a 4-km resolution (NMM4), were also available to HWT. These forecasts all started from 00 UTC each day, and ran up to 36 hours. Different physics options were used by these forecasts. These forecasts acted, in a way, as additional members of a larger ensemble, and the diversity of these forecasts provided additional probabilistic guidance to the forecasters.

Parallel to the N-AWIPS system, graphical plotting and ensemble post-processing were also performed by CAPS, with the graphical products generated as soon as the model outputs are created and posted on the web at http://www.caps.ou.edu/wx/spc. These graphical products were produced using ARPSPLT, run in MPI mode, after WRF outputs were converted to the ARPS grid via WRF2ARPS. All input and output data were achieved in the mass store of PSC, and will be used for detailed post-real time analysis.

Table 1. Ensemble member configuration

member	IC	BC	microphysics	PBL scheme
CN	21Z NAMa	18Z NAMf	WSM6	MYJ
N1	CN – arw_pert	21Z SREF arw_n1	Ferrier	MYJ
P1	CN + arw_pert	21Z SREF arw_p1	Thompson	MYJ
N2	CN – nmm_pert	21Z SREF nmm_n1	Thompson	YSU
P2	CN + nmm_pert	21Z SREF nmm_p1	WSM6	YSU
PH1	21Z NAMa	18Z NAMf	Thompson	MYJ
PH2	21Z NAMa	18Z NAMf	Ferrier	MYJ
PH3	21Z NAMa	18Z NAMf	WSM6	YSU
PH4	21Z NAMa	18Z NAMf	Thompson	YSU
PH5	21Z NAMa	18Z NAMf	Ferrier	YSU

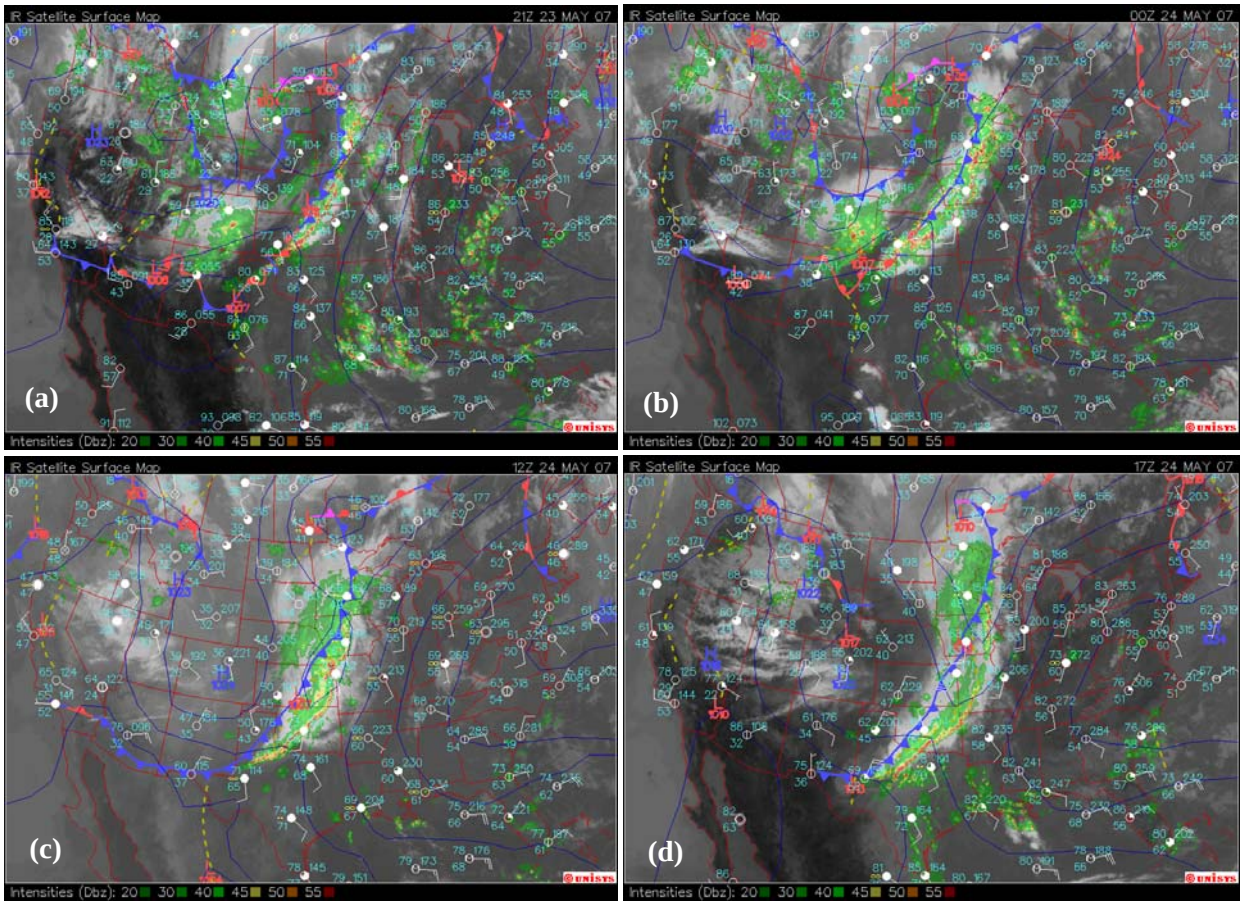

Fig. 2. Surface weather analyses with IR satellite imagery and radar reflectivity overlaid, for 21 UTC, 23 May (a), and 00 UTC (b), 12 UTC (c) and 17 UTC (d) of 24 May 2007. Maps courtesy of Unisys.

3. Forecast Examples

Since detailed analyses of the realtime forecasts have yet to be completed, in this paper, we will only present forecasts from one of the days for illustration purpose. Some preliminary analysis of the ensemble forecasts, including ensemble statistics and a comparison of individual forecasts for the prefrontal squall line case of May 23-25, can be found in a companion paper, Kong et al. (2007). A discussion on the WRF model guidance during the Spring Experiment, especially those of NCEP NMM4 and NSSL ARW4, for the 4 May 2007 Greensburg, Kansas tornadic supercell case can be found in Weiss et al. (2007). We will present here forecasts of a squall line case, that was initialized at 21 UTC, 23 May and run through 06 UTC, 25 May 2007.

a. The 23-25 May 2007 squall line case

At 21 UTC, 23 May, a well defined, solid, line of convection was found extending from Texas panhandle trough central Kansas, into Iowa then Wisconsin, immediately ahead of a weak surface front (Fig. 2a). A surface low was located at the U.S.-Canada border of North Dakota while a high was centered off the east coast of Maine. The return flows of the high brought moist air from the Gulf of Mexico into the Central Great Plains Fig. 2a). After 22 UTC, this line of convection became less organized, and some scattering was found with the convection along the middle section of the line by 00 UTC, 24 May (Fig. 2b).

During the next 3 hours up 03 UTC, this line of convection went through reorganization, and by 04 UTC, an essentially solid line was re-established. This squall line continued to propagate eastward, and started to develop a trailing stratiform precipitation region with a secondary reflectivity maximum behind the leading convection by 12 UTC at the central portion in eastern Kansas (Fig. 2b). By 17-18 UTC, this stratiform region had shifted to the southern section of the squall line, into south-central Oklahoma (Fig. 2b and Fig. 3i). After 18 UTC, the middle section of the squall line within Missouri started to disintegrate and disappeared completely by 00 UTC, 25 May (Fig. 3k), while the southern section progressed mostly southward, with the main convection remaining at southwestern Taxes near the Mexico border by 06 UTC (Fig. 3m). By this time, only some residual precipitation was seen with the northern portion of the squall line over the Great Lakes (Fig. 3m).

b. Deterministic predictions

The overall evolution of this precipitation system was captured reasonably well by the 2 km WRF and most members of the 4 km ensemble, although significant differences from the observations and among the forecasts themselves are found in the details.

Within two hours after the initialization, the 2 km grid span up the convection to similar intensities as observed in terms of the simulated reflectivity, and this can be seen from Fig. 3b at 3 hours, valid at 00 UTC May 24. The model captured the general line of convection extending from Texas panhandle through Wisconsin, but there are significant differences in the detailed structures in the panhandle area and in southeastern Kansas and Iowa. The general patterns of precipitation along a secondary cold front (Fig. 2b) and in eastern Colorado that originated from afternoon orographic forcing were also captured. Considering that the model initial condition contained no convective-scale data, the quick spinning up of pre-existing, well organized, precipitation within two hours of forecast is very encouraging. The model was able to do so, apparently because of the presence of strong synoptic and mesoscale forcings that seemed to have been reasonably captured in the initial conditions. Interestingly, the prediction of the control member of the 4 km ensemble look very similar at this time (not shown), suggesting that small-scale details had not had an opportunity to exert their influence. In fact, there were no near-grid-scale structures in the ICs of either 2 or 4 km grid because the ICs came from the 12 km NAM analysis. Had high-resolution radar data been assimilated into the ICs, larger differences between the 2 and 4 km forecasts should be expected.

As pointed out earlier, during the next few hours, the observed convection went through a phase of reorganization, and ended up with a line whose middle section located in Kansas lagged somewhat behind other sections (Fig. 3e). This detailed behavior was not, however, reproduced in the 2 km WRF model (Fig. 3f) or in any member of the 4 km ensemble (not shown).

Over the next 12 hours, the observed squall evolved through its mature stage, developing into a classic squall line with intense leading edge convection and a trailing stratiform precipitation region (Fig. 3e,g,i). At 18 UTC, the squall was most intense within Oklahoma and northern Texas.

The squall line in the 2 km WRF forecast reached its maximum intensity and organization at 18 UTC (Fig. 3i) with a rather accurate positioning at the southern section. Its middle section was displaced northwestward, into eastern Kansas rather than going through central Missouri as observed. It was partly caused by the structural differences in the predicted convection from observation in the earlier hours. Between 12 and 15 UTC, the middle portion of the line within Oklahoma was too weak in the prediction (Fig. 3f,h) and the leading edge of convection was already lagging somewhat. Between 15 and 18 UTC, the predicted leading convection in this section dissipated while the secondary convection behind it intensified, resulting in an apparent westward displacement of line at this time.

Over the next 6 hours, the model correctly predicted the weakening of the middle section of the squall line and the transition of its southern section into a more east-west orientation (Fig. 3l,n). Preliminary analysis indicates that after 18 UTC, the low-level southerly flows east of the squall line were part of the anti-cyclonic circulation that did not pass over the Gulf, and therefore did not contain as much moisture as the earlier southerly flows feeding the Oklahoma-Kansas region. With the help of Gulf moisture, the convection at the southern portion remained active until 06 UTC, 25 May, when the model runs ended (Fig. 3n). After this time, the observed convection weakened in central Texas, apparently because of the lack of synoptic scale support (not shown).

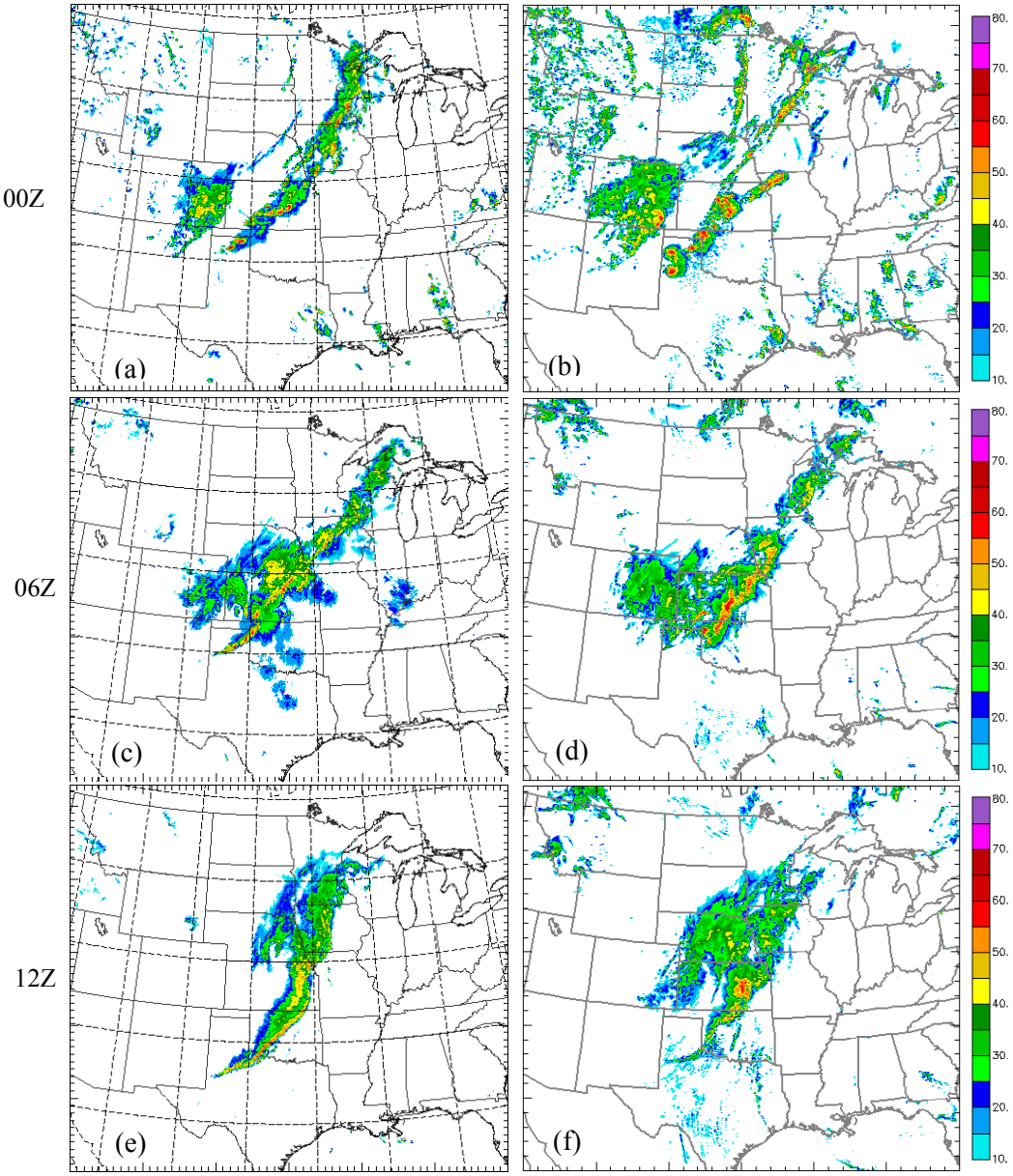

Fig. 3. Observed composite reflectivity (left column) and forecast composite reflectivity of the 2 km grid (ARW2) starting from 21 UTC, 23 May 2007 (right column), valid at 00, 06, 12, 15, 18 UTC, 24 May, and at 00 and 06 UTC, 25 May 2007.

Throughout the 2 km forecasts and in all 4-km ensemble members, the model failed to predict the secondary maximum associated with the stratiform precipitation region – this is a common problem with squall line prediction (e.g., Xue et al. 1996). On the other hand, as pointed out earlier, the rather successful prediction of the overall pattern and evolution of this squall line case, for up to 33 hours, on both 2 and 4 km WRF grids, is encouraging.

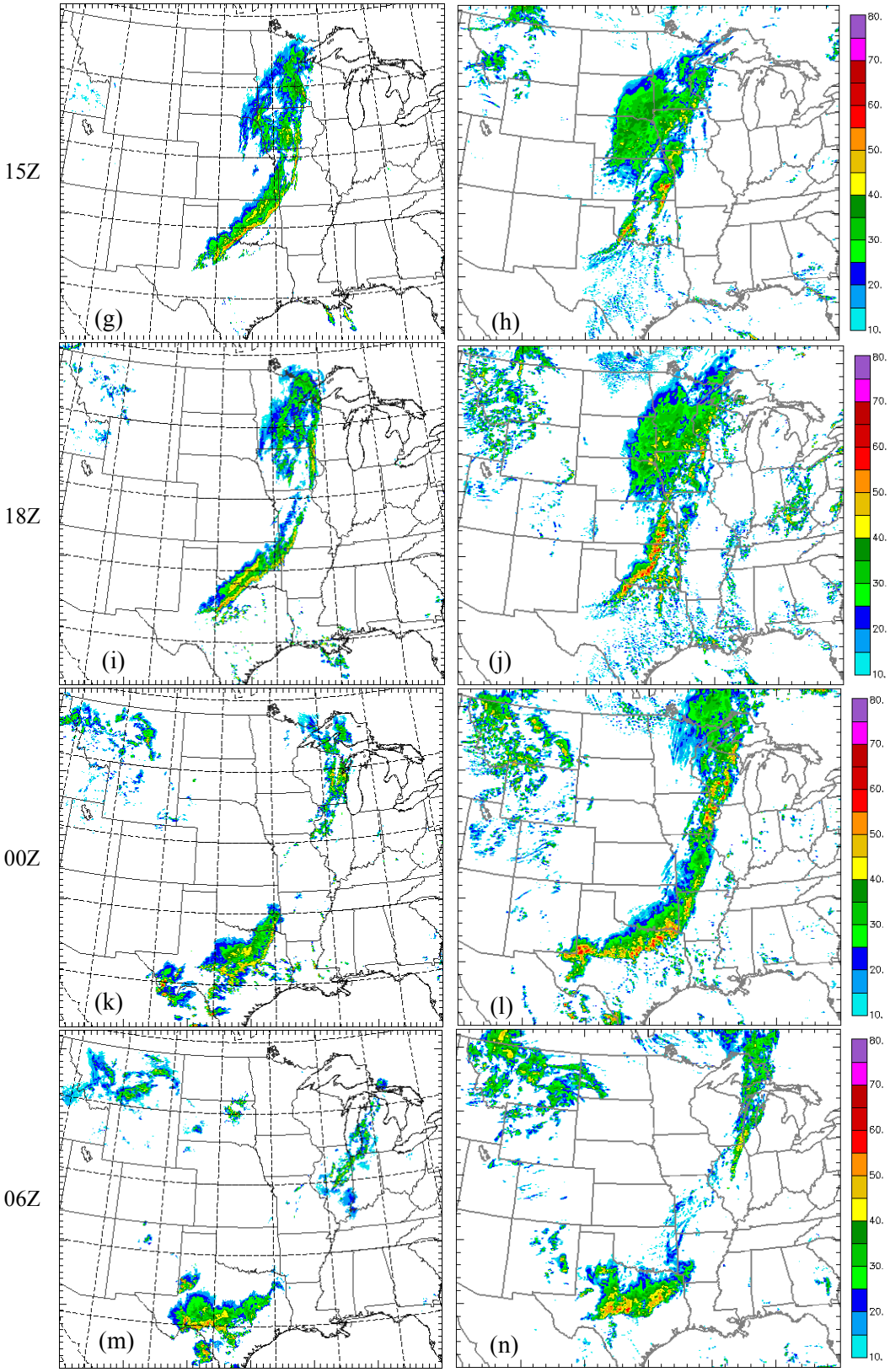

Fig. 3. Continued.

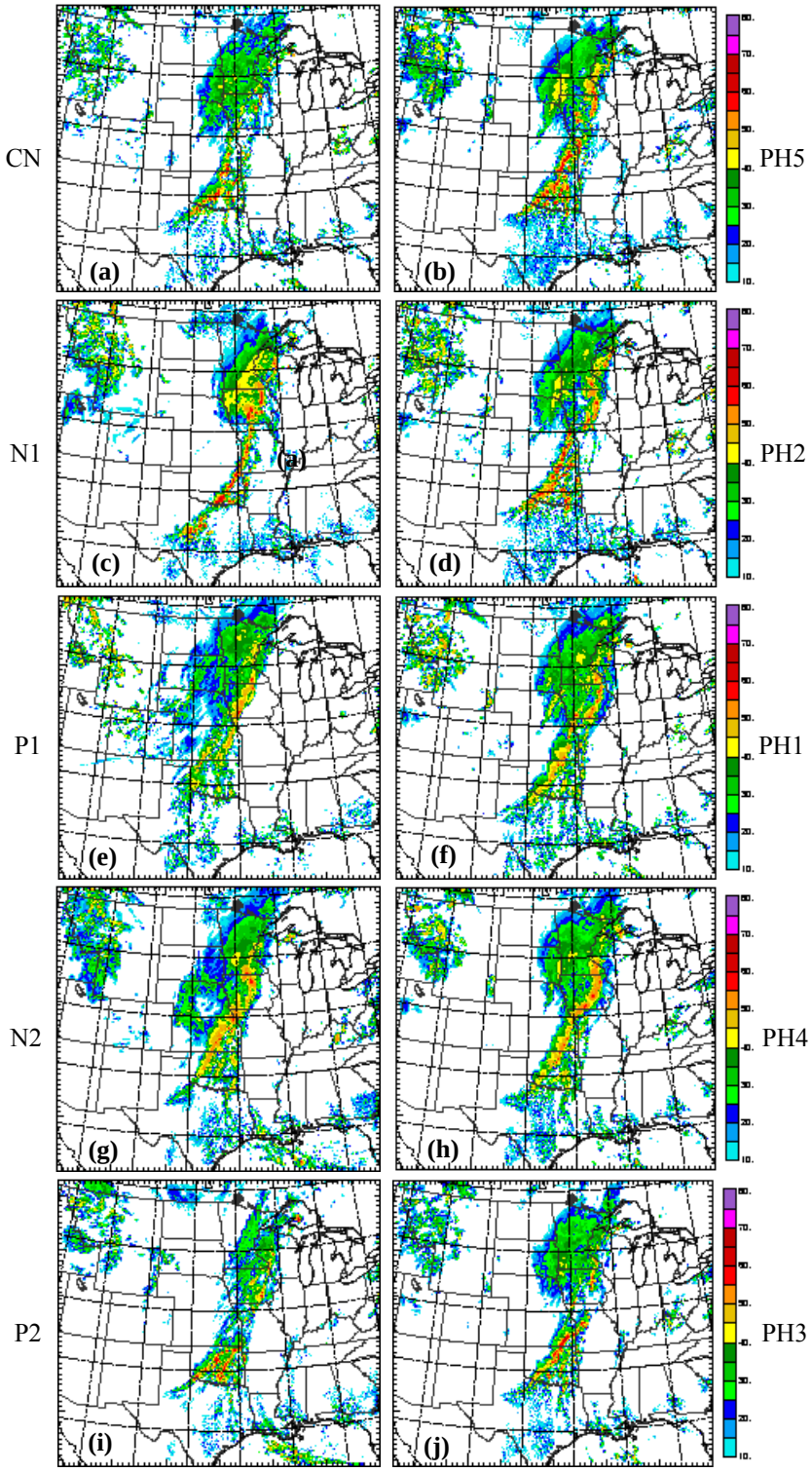

Fig. 4. Postage stamp view of 21-hour forecast composite reflectivity fields from ten members of the 4-km ensemble, valid at 1800 UTC, 24 May 2007. Starting from second raw, the side by side members have the same physics. Control member (CN) and the physics members (PH1-PH5) have the same initial (2100 UTC, 23 May 2007 NAM analysis) and boundary conditions (NAM forecasts of 1800 UTC cycle of 23 May 2007), while P1, N1 and P2 and N2 have perturbed initial and boundary conditions.

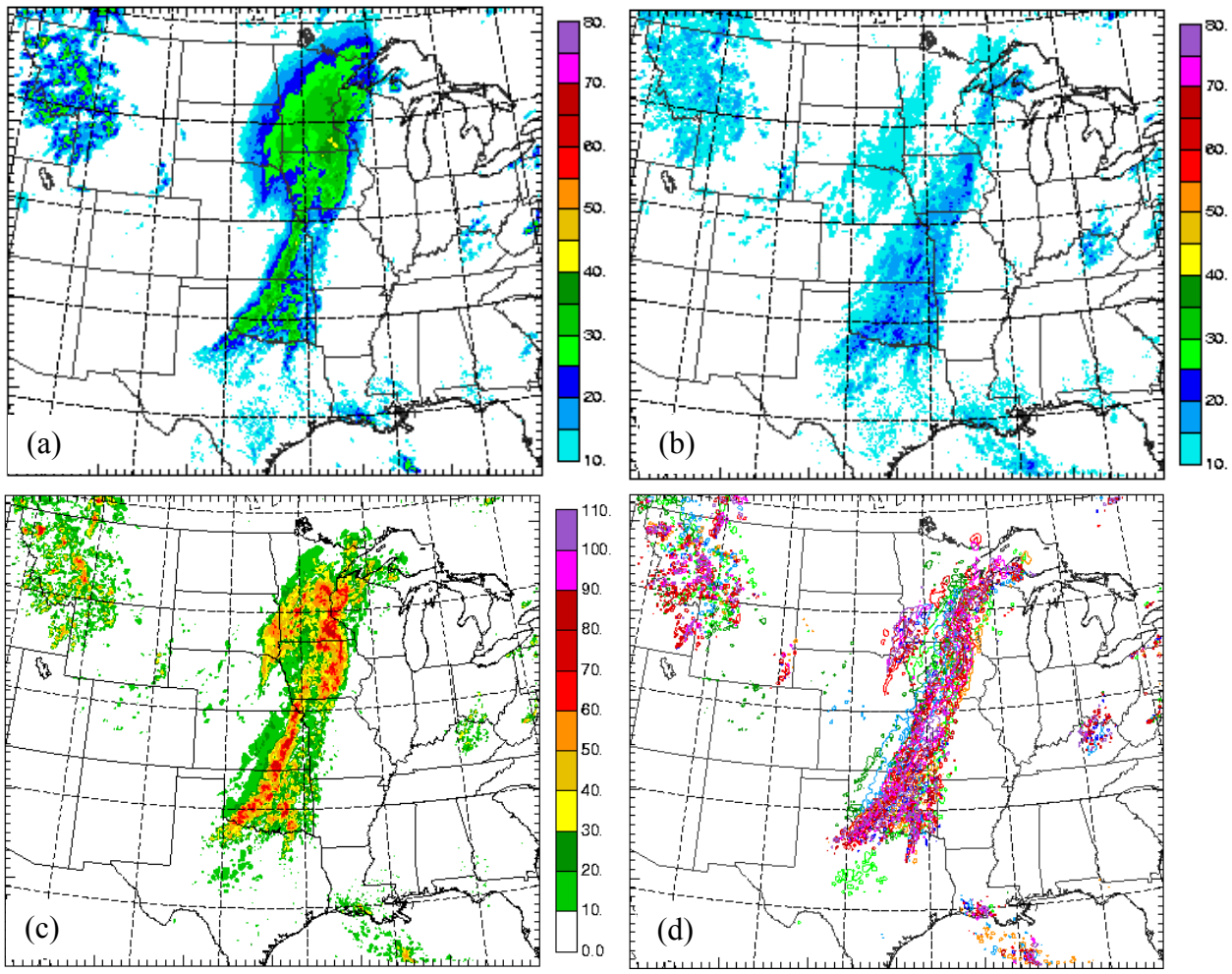

Fig. 5. Forecast composite reflectivity ensemble mean (a) and spread (b), and ensemble-derived probability of composite reflectivity exceeding 35 dBZ (c) and the 'spaghetti' plot of 40 dBZ composite reflectivity contours, valid at 18 UTC, 24 May 2007, corresponding to 21 hour forecast.

c. Ensemble forecasts

Fig. 4 shows a postage stamp view of the 21-hour forecast composite (column maximum) reflectivity (simply reflectivity hereafter) fields from ten members of the 4-km ensemble, valid at 1800 UTC, 24 May 2007, when the observed squall line was at its mature stage with pronounced trailing stratiform precipitation (Fig. 3i). The plots are arranged so that the members in the same raw used the same physics, except for the first raw that contains the control member (CN) and physics-perturbation member 5 (PH5). The control member (CN) and all physics members (PH1-PH5) used the same IC and BCs, while P1, N1 and P2 and N2 had perturbed IC and BCs.

A general impression of the results shown in Fig. 4 and those of many other days (not shown) is that the N and P members that contained both IC/BC and physics perturbations usually exhibit larger spread than among the pure-physics perturbation members themselves, which is expected. A more interesting result is that the differences between members with different physics (right column and control in Fig. 4) tend to be smaller than the differences between members of the same physics (side by side pairs in Fig. 4) but different ICs and BCs, especially in terms of the convective line position. For example, the position of the primary convective line within Oklahoma is almost exactly the same among all physics (PH1-PH5) and control (CN) members, while the line position among the four N and P members change greatly. The large-scale perturbations of SREF that were generated through breeding must have altered the synoptic and mesoscale flow patterns to cause the larger spread in the position of convection, while the convection developing in the same large scale environment in the physics perturbation members tends

to differ mainly in the intensity and organization at the convective scale. These results suggest that to account for uncertainties in both convective and larger scales, both IC/BC and physics perturbations should be included in the ensemble system. For spring 2007, we deliberately chose to exclude IC/BC perturbations in the physics perturbation members, to help meet our additional goal of identifying systematic behaviors of various WRF physics packages.

Among all members, N1 exhibits the best line organization of convection at18 UTC (Fig. 4c) while P1 exhibits least organization (Fig. 4e). Rather large differences are also found between N2 and P2 at this time (Fig. 4g,i). In terms of the squall line position at 18 UTC, N1 seems to do the best job, among all ensemble members and including the 2 km high-resolution forecast. N1 does over-predict the intensity of convection in the central position, and also lacks the stratiform precipitation. N2 and P2, similar to CN, predict a double line structure inside Okalahoma that is not real.

Fig. 5 shows the ensemble mean and spread of forecast reflectivity, the ensemble-derived probability of reflectivity exceeding 35 dBZ and the 'spaghetti' plot of 40 dBZ reflectivity contours, valid at 18 UTC. Because we are dealing with spatially discrete convective-scale features here, the magnitude of the ensemble mean is not very meaningful – the ensemble mean will almost surely underestimate the intensity. The only region where the mean reflectivity exceeds 40 dBZ is in southeast Minnesota (Fig. 5a); there, the cold front consistently anchored the precipitation location among most members (Fig. 2d). The maximum mean reflectivity remains in the 30-40 dBZ range along a line, and the positioning of the middle portion of this line is no better than that of the control or 2 km forecast.

Fig. 5b shows that the spread of reflectivity has values between 20 and 25 dBZ along much of the line, indicating significant uncertainties at the convective scale. Fig. 5c shows that the pattern of ≥50% probability of reflectivity exceeding 35 dBZ matches that of high ensemble mean reflectivity very well, which therefore has a similar position error. The 'spaghetti' plot in Fig. 5d suggests more spread in the position than the probability field suggests and is therefore more indicative of position uncertainty. In general, ensemble prediction for the convective scale remains a very new field and the evaluation of the ensemble forecast at this scale still requires much research.

We do want to point out here that for all members, the simulated reflectivity was calculated from the predicted hydrometeors using the same reflectivity formula that is based on the Lin microphysics scheme with its default intercept and density parameters. Our calculations for later cases using formulas consistent with the individual microphysics schemes show that the Lin formula generally over-estimates the composite reflectivity, with most difference found at the upper levels related to the ice species. Therefore the quantitative comparison among the reflectivity fields should be viewed with caution.

4. Future Plan

The output from the ensemble and high-resolution forecasts, saved at hourly intervals, for more than 6 weeks, provide us an unprecedented opportunity for investigating many aspects of convective-scale prediction. These include the performance and behavior of the ensemble system using mixed initial/boundary condition and physics perturbations, and the relative performance and behavior of microphysics and PBL schemes tested. Detailed post-real time or retrospective analyses will be carried out by ourselves and by collaborators and the results will guide the refinement of our experiments over next two years.

The planned enhancements for the future years include the addition of WRF-NMM model and the assimilation of WSR-88D radar data and other special and local observations into the control initial conditions. The data assimilation will be initially done using the ARPS 3DVAR and cloud analysis and later using the NCEP GSI system. The ensemble system for the next year will likely to employ a full mix of IC, BC and physics perturbations as well as more than one dynamic core. The IC perturbations may employ an ETKF-based method (Wang and Bishop 2003). When computational resources permit, we will also attempt higher horizontal resolutions. The goal is to address the scientific questions posed in introduction as much as possible, given inevitable practical constraints.

5. Afterthoughts on an Optimal Prediction/ Assimilation System

We offer here some thoughts on the convective-scale predictability and potential optimal assimilation/prediction systems under practical computational constraints. The rather successful prediction of the overall pattern and evolution of this squall line case obtained at 2-4 km resolutions is very encouraging, especially considering that we are examining convective-scale predictions for up to 33 hours. Such results have implications to our understanding of convective-scale predictability and in this particular case that of an organized mesoscale convective system. Similar predictability was shown by Xue et al. (2001) for a prefrontal squall line of January 1999. On the other hand, if we focus on convection at individual cell scale, the predictions obtained here can not be considered good as the specific details usually do not agree with the observations. This is true of the forecasts in the first few

hours also, during which convective-scale data assimilation will be necessary and promises to allow short-range predictions down to the individual cell level. The fact that the 4 km control prediction agrees with that of 2 km grid much more so than with other members of the 4 km ensemble suggests that for forecasts of the ranges (beyond 12 hours) considered here, a 4 km grid may be as good as a 2-km grid, given many of the IC and model uncertainties.

We envision that an optimal ensemble-based data assimilation and prediction system will consist of a lower-resolution (LR, ~ 4 km) ensemble of about 50 members, with continuous data assimilation cycles of up to the WSR-88D volume scan frequency (~ every 5 minutes) performed on a high-resolution (HR) grid of 1 km resolution or higher, as well as on the LR grid which provides ensemble IC perturbations. These perturbations can be transformed using ETKF to maximize the independent perturbation directions represented (Wang et al. 2004). High-resolution predictions are launched periodically, at, e.g., hourly intervals, and predict for a shorter range (~ 6 hours) until most of the benefit of high resolution diminishes. The HR prediction and assimilation system provides improved ensemble means of analysis and prediction for use by the LR ensemble. The LR ensemble predictions are carried out to a much longer range (~ 48 hours) to provide probabilistic forecast information. In principle, beyond this range, the resolution of the ensemble can be further decreased because fine-scale details lose their predictability beyond this range. However, the need to avoid cumulus parameterization dictates of use of a convection-allowing resolution, hence this ~ 4 km resolution should be maintained when a longer range prediction is desired (which usually also requires a large model domain).

In a sense, such an ensemble prediction/data assimilation system is an extension of the dual-resolution ensemble data assimilation approach proposed by Gao and Xue (2007), which has been shown to work well for the assimilation of simulated radar data. Because of the need to include observational data representing different scales of atmospheric motion, a hybrid framework combining 3DVAR and ensemble-derived background error statistics may be most effective (Wang et al. 2007), because of the benefit of more reliable remote correlations represented within the 3DVAR error statistics.

Acknowledgement: This research was mainly supported by a grant to CAPS from the NOAA CSTAR program. Supplementary support was also provided by NSF ITR project LEAD (ATM-0331594). Suggestions and input from NCAR scientists Drs. Jimy Dudhia, Morris Weisman, Greg Thompson and Wei Wang on the WRF model configurations were every helpful. The realtime predictions were performed at the Pittsburgh Supercomputing Center (PSC). David O'Neal of PSC provided ever present technical and logistic support that was essential to the success of the forecast experiment. Support from Dr. James Kimpel of NSSL, Joseph Schaeffer of SPC and Geoff DiMego of NCEP/NMC are also greatly appreciated.

References

Du, J., J. McQueen, G. DiMego, Z. Toth, D. Jovic, B. Zhou, and H. Chuang, 2006: New dimension of NCEP Short-Range Ensemble Forecasting (SREF) system: Inclusion of WRF members. Preprint, WMO Expert Team Meeting on Ensemble Prediction System, Exeter, UK, 5pp.

Gao, J., M. Xue, K. Brewster, and K. K. Droegemeier, 2004: A three-dimensional variational data analysis method with recursive filter for Doppler radars. *J. Atmos. Ocean. Tech.*, **21,** 457-469.

Gao, J. and M. Xue, 2007: An efficient dual-resolution approach for ensemble data assimilation and tests with assimilated Doppler radar data. *Mon. Wea. Rev.,* Conditionally accepted.

Hu, M. and M. Xue, 2006: Impact of configurations of rapid intermittent assimilation of WSR-88D radar data for the 8 May 2003 Oklahoma City tornadic thunderstorm case. *Mon. Wea. Rev.,* Accepted.

Hu, M., M. Xue, and K. Brewster, 2006a: 3DVAR and cloud analysis with WSR-88D level-II data for the prediction of Fort Worth tornadic thunderstorms. Part I: Cloud analysis and its impact. *Mon. Wea. Rev.*, **134,** 675-698.

Hu, M., M. Xue, J. Gao, and K. Brewster, 2006b: 3DVAR and cloud analysis with WSR-88D level-II data for the prediction of Fort Worth tornadic thunderstorms. Part II: Impact of radial velocity analysis via 3DVAR. *Mon. Wea. Rev.*, **134,** 699-721.

Kain, J. S., S. J. Weiss, D. R. Bright, M. E. Baldwin, J. J. Levit, G. W. Carbin, C. S. Schwartz, M. Weisman, K. K. Droegemeier, D. Weber, and K. W. Thomas, 2007: Some practical considerations for the first generation of operational convection-allowing NWP: How much resolution is enough? Preprints, 22nd Con. Wea. Ana. Forecasting/18th Conf. Num. Wea. Pred., Park City, UT, Amer. Meteor. Soc., CD-ROM 3B5.

Kong, F., M. Xue, D. Bright, M. C. Coniglio, K. W. Thomas, Y. Wang, D. Weber, J. S. Kain, S. J. Weiss, and J. Du, 2007: Preliminary analysis on the real-time storm-scale ensemble forecasts produced as a part of the NOAA hazardous weather testbed 2007 spring experiment. 22nd Conf. Wea. Anal. Forecasting/18th Conf. Num. Wea. Pred., Salt Lake City, Utah, Amer. Meteor. Soc., CDROM 3B.2.

Wang, X. and C. H. Bishop, 2003: A comparison of breeding and ensemble transform Kalman filter ensemble forecast schemes. *J. Atmos. Sci.*, **60,** 1140-1158.

Wang, X., C. H. Bishop, and S. J. Julier, 2004: Which is better, an ensemble of positive–negative pairs or a centered spherical simplex ensemble? *Mon. Wea. Rev.*, **132,** 1590–1605.

Wang, X., C. Snyder, and T. M. Hamill, 2007: On the theoretical equivalence of differently proposed ensemble–3DVAR hybrid analysis schemes. *Mon. Wea. Rev.*, **135,** 222–227.

Weiss, S. J., J. S. Kain, D. R. Bright, J. J. Levit, G. W. Carbin, M. E. Pyle, Z. I. Janjic, B. S. Ferrier, J. Du, M. L. Weisman, and M. Xue, 2007: The NOAA Hazardous Weather Testbed: Collaborative testing of ensemble and convection-allowing WRF models and subsequent transfer to operations at the Storm Prediction Center. 22nd Conf. Wea. Anal. Forecasting/18th Conf. Num. Wea. Pred., Salt Lake City, Utah, Amer. Meteor. Soc., CDROM 6B.4.

Xue, M., K. K. Droegemeier, D. Wang, and K. Brewster, 1996: Prediction and simulation of a multiple squall line case during VORTEX-95. Preprint: 18th Conf. on Severe Local Storms, 19-23 Feb., San Francisco, CA., Amer. Meteor. Soc.

Xue, M., K. K. Droegemeier, V. Wong, A. Shapiro, K. Brewster, F. Carr, D. Weber, Y. Liu, and D. Wang, 2001: The Advanced Regional Prediction System (ARPS) - A multi-scale nonhydrostatic atmospheric simulation and prediction tool. Part II: Model physics and applications. *Meteor. Atmos. Phys.*, **76,** 143-166.